Title:

Energy localisation and frequency analysis in the locust ear

Short title:

Efficient hearing in the locust

Author affiliation:

Robert Malkin[a,1], Thomas R. McDonagh[b,1], Natasha Mhatre[a, 1], Thomas S. Scott[c], Daniel Robert [a,2]

[a] School of Biological Sciences, University of Bristol, Woodland Road, Bristol, BS8 1UG, UK

[b] Present Address: Laboratory of Cellular Biophysics, The Rockefeller University, 1230 York Avenue, New York, NY 10065, USA

[c] Interface Analysis Centre, University of Bristol, 121 St. Michael's Hill Bristol, BS2 8BS, UK

[1] The authors contributed equally to this work and are listed alphabetically

[2] To whom correspondence should be addressed: D.Robert@bristol.ac.uk

Keywords:

tympanum | travelling flexural wave | tension | energy localisation | frequency discrimination

Abstract

Animal ears are exquisitely adapted to capture sound energy and perform signal analysis. Studying the ear of the locust, we show how frequency signal analysis can be performed solely by using the structural features of the tympanum. Incident sound waves generate mechanical vibrational waves that travel across the tympanum. These waves shoal in a tsunami like fashion, resulting in energy localisation that focuses vibrations onto the mechanosensory neurons in a frequency dependent manner. Using finite element analysis, we demonstrate that two mechanical properties of the locust tympanum, distributed thickness and tension, are necessary and sufficient to generate frequency-dependent energy localisation.

1 Introduction

All auditory systems convert airborne sounds into vibrations of specialised anatomical structures. This motion is then transduced into nerve impulses for processing by the central nervous system. The mammalian ear has distinct locations for each of these tasks. The eardrum receives acoustic energy that is coupled via the middle and inner ear to hair cells in the cochlea, the site of transduction. In the mammalian ear, low energy density sound signals are conducted through the ossicles in the middle ear, an impedance conversion device that greatly facilitates the ingress of acoustic energy into the cochlea. The capture of acoustic energy by the fluid-filled ears of mammals thus requires elaborate structural mechanics (1). Insects exhibit auditory systems that are structurally simpler, but still achieve complex signal analysis (2,3). In locusts, both acousto-mechanical conversion and information processing are readily performed by the tympanum; a membrane endowed with unconventional structural and material specialisations (4), that performs limited discretisation of sound waves into distinct frequency components (5). The histological architecture and micromechanics that endow the microscale ears of insects with high sensitivity and frequency selectivity are still poorly understood, yet they constitute valuable evolutionary solutions to long-standing problems of sound detection.

The locust tympanal membrane (TM)

(

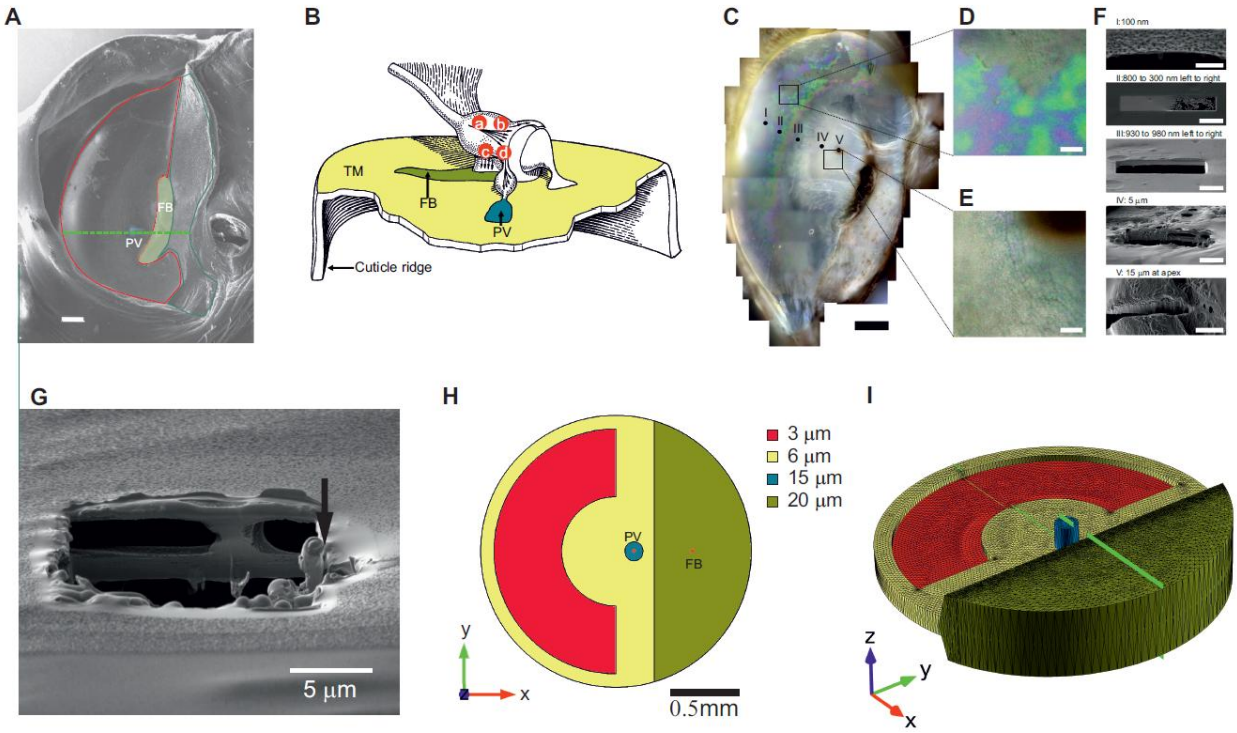

Figure 1) serves as a good model to explore frequency analysis in micro scale auditory systems; it is experimentally amenable and has identifiable structural features that enable computational modelling. The kidney shaped membrane (2.5 x 1.5 mm in size) is supported by a rigid cuticular rim around its perimeter, and presents two distinct regions; a thin

and transparent membrane (delineated in red,

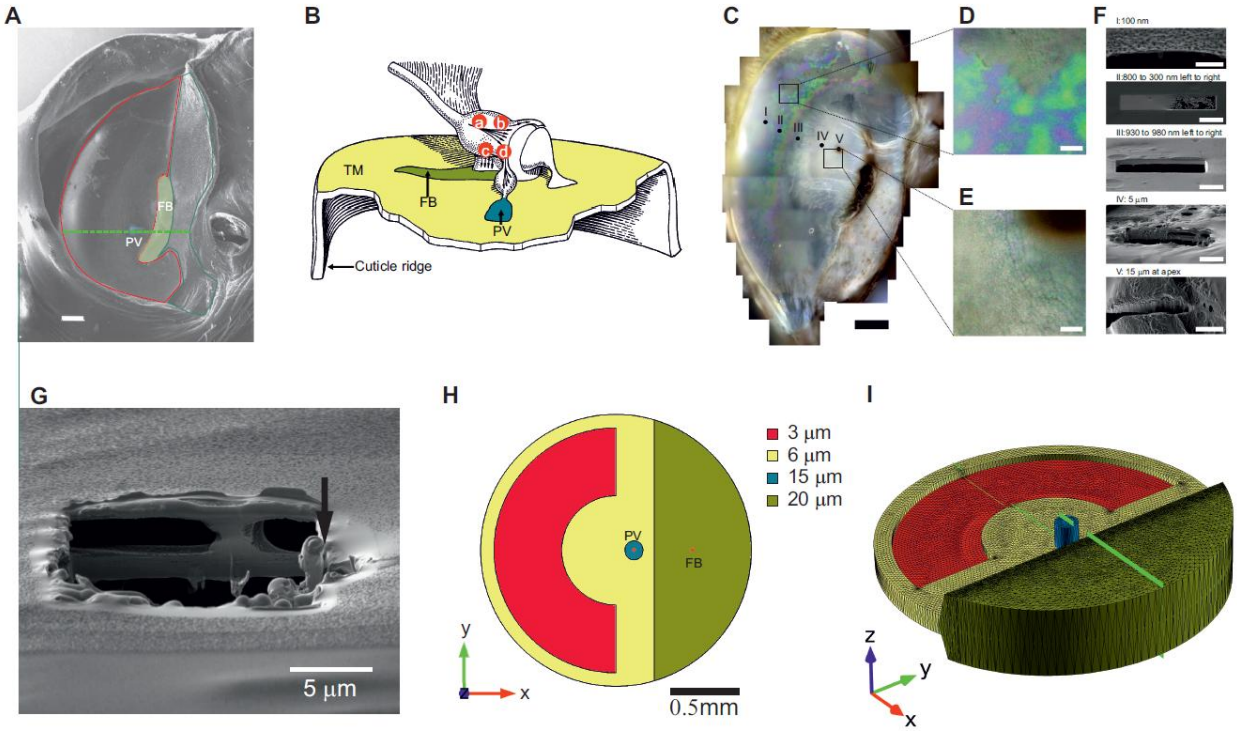

Figure 1A), and a thick membrane (delineated in green) where the folded body (FB) and the pyriform vesicle (PV) are located. The FB and the PV are connected on the inner surface to Müller's organ, which contains about 120 mechanoreceptor cells distributed in four distinct groupings (a-d) [a, b, c: connected to the FB, d connected to the PV] shown in

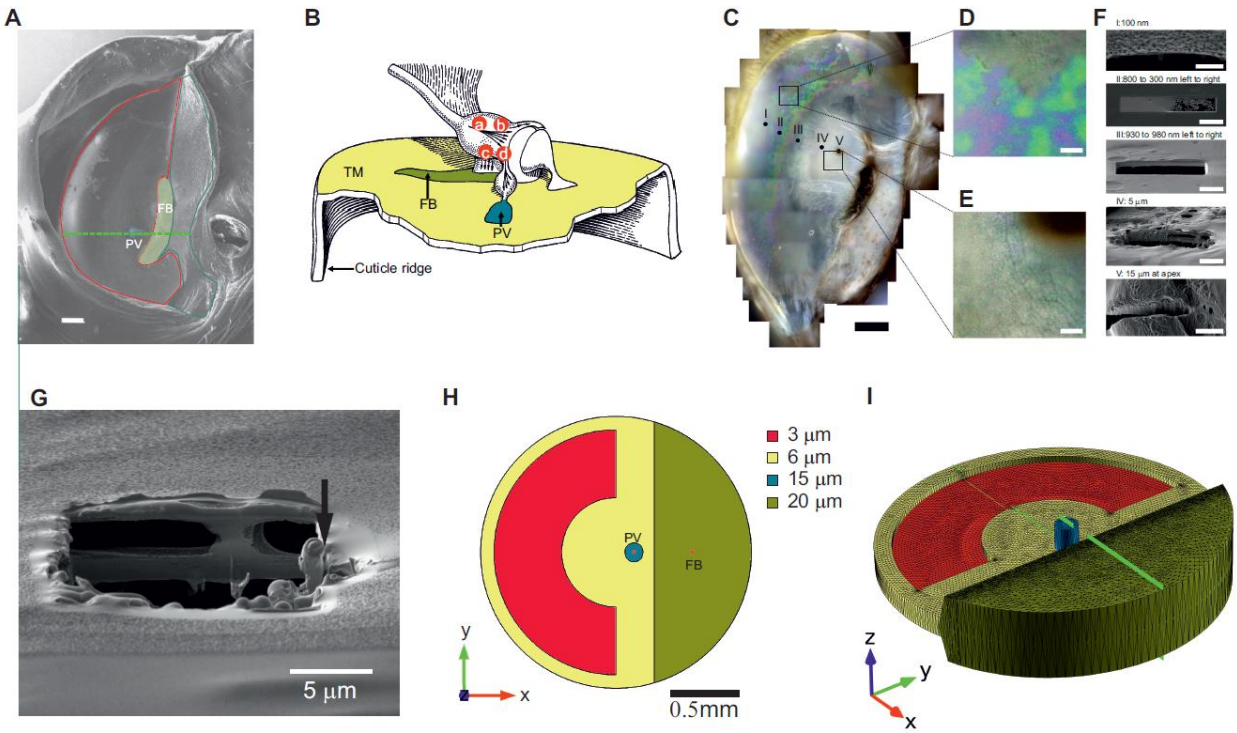

Figure 1B, (6). The auditory nerve, connected to Müller's organ, in turn conveys acoustic information to the central nervous system (7,8). The TM therefore performs the complete mechanical function of coupling

airborne acoustic energy to the nervous system. The locust has an interesting mechanical response to impinging sound waves. Low frequencies (<10 kHz) elicit travelling flexural waves of the TM that cause mechanical deflection at the both the FB and PV. In contrast, higher sound frequencies (>10 kHz) only deflect the PV (9). Phenomenologically, this frequency response is achieved by waves travelling in a frequency dependent manner to different mechanoreceptors attached to the two regions (9).
Understanding the vibrational dynamics of the TM is critical to understanding how the ear collects acoustic energy and then distributes it within the TM structure to produce mechanical oscillations at different mechanoreceptor sites. Here, we characterise the geometry and vibrations of the TM, using enhanced methods, derive analytic models and predictions for TM behaviour and, using finite element analysis (FEA), we identify the TM features required for energy localisation and frequency discretisation, namely a heterogeneous thickness distribution and tension.

2 The locust tympanum as a membrane or stiff plate

Two distinct physical properties strongly influence the mechanical behaviour of homogeneous membranes; tension and stiffness (10). The locust TM is known to be under tension, as demonstrated by the fact that a linear cut readily relaxes into an oval opening (11). Also, changes in the pressure in the air sac behind the TM modulate the frequency response of the TM and changing the sensitivity of receptor cells (12), presumably through alteration of membrane tension. The membrane is likely to have non-negligible bending stiffness, especially in the thick region around the PV and FB. Measuring membrane tension and stiffness directly using local probe methods (atomic force microscopy) has proven very unreliable, due to the uncontrollable adhesion of the probe to the sample during measurement (McDonagh & Robert, pers. obs.).
Hence, the influence of tension and stiffness on flexural wave velocity were explored using theoretical predictions of vibration behaviour. Predictions were derived for two contrasting models of TM dynamics:
(1) Membrane Model - a membrane with uniform in-plane tension and negligible stiffness.
(2) Stiff Plate Model - a membrane with isotropic stiffness and negligible tension.
Using wave-equations for each model, we derive an equation for the propagation velocity of the travelling flexural wave which described dependence on tension T, thickness h, density μ, Young's Modulus E, Poisson's Ratio ν, and angular frequency ω (See Supplementary Note 1 for derivations) (13).

1 - Membrane
$$v = \sqrt{\frac{T}{h\mu}} \tag{1}$$

2 - Stiff Plate
$$v = \left(\frac{E}{12\mu(1-\nu^2)}\right)^{1/4} \sqrt{h\omega} \tag{2}$$

Therefore, if the locust membrane is a tension dominated system, the velocity of the travelling flexural wave will decrease with increasing thickness of the membrane, i.e. travelling flexural waves will slow down as they approach the PV. If the stiff plate model dominates, the model predicts that the velocity of the wave will increase as it approaches the PV. Measuring the change in travelling flexural wave velocity during propagation allows us an experimental way to distinguish between the two possibilities.

3 Methods

3.1 Animals

Experiments were performed on 7 adult male or female *Schistocerca gregaria* Forskål. The animals (supplied by Blades Biological,Cowden, UK) were kept in standard conditions (temperature: 24-26° C, relative humidity: 60-70%). Animals remained alive throughout the experiment but were anaesthetised by injection of glutamate in saline solution (approx. 10% by volume) to prevent abdominal breathing, which causes large and slow movements of the TM resulting in temporary loss of signal from the LDV. Preliminary experimental work showed that the use of glutamate had no observable effect on the membrane response. To allow optical access to the tympanal ear during laser vibrometry measurements, the wings were removed. The animals were fixed, ventrum down, to a horizontal brass bar and held firm by a looped wire around the animal and the bar. The brass bar was orientated such that the animal could be held at a slight angle from the perpendicular to the laser beam to fully expose the tympanal ear. The intact right ear of each animal was examined

(

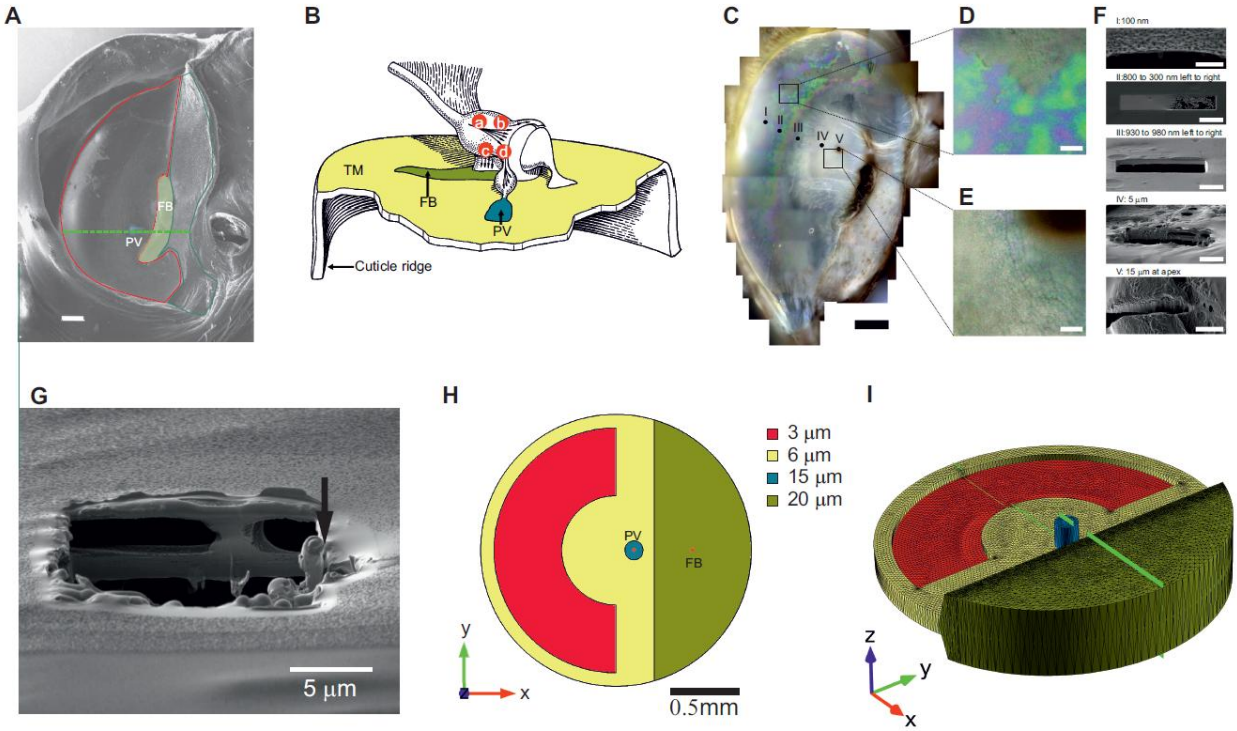

Figure 1C).

3.2 Coloured Newton ring interferometry

Reflected illumination creates optical interference between light reflected from the top and bottom surfaces of the TM. Using coloured Newton ring interferometry allows us to accurately visually identify the distribution of thin regions of the membrane. Note that membrane thickness quantification using Newton rings is not possible here as it requires knowledge of the local refractive index. The technique clearly reveals the geometric distribution of both the thin concentric region of the membrane and the opaque thick region

(

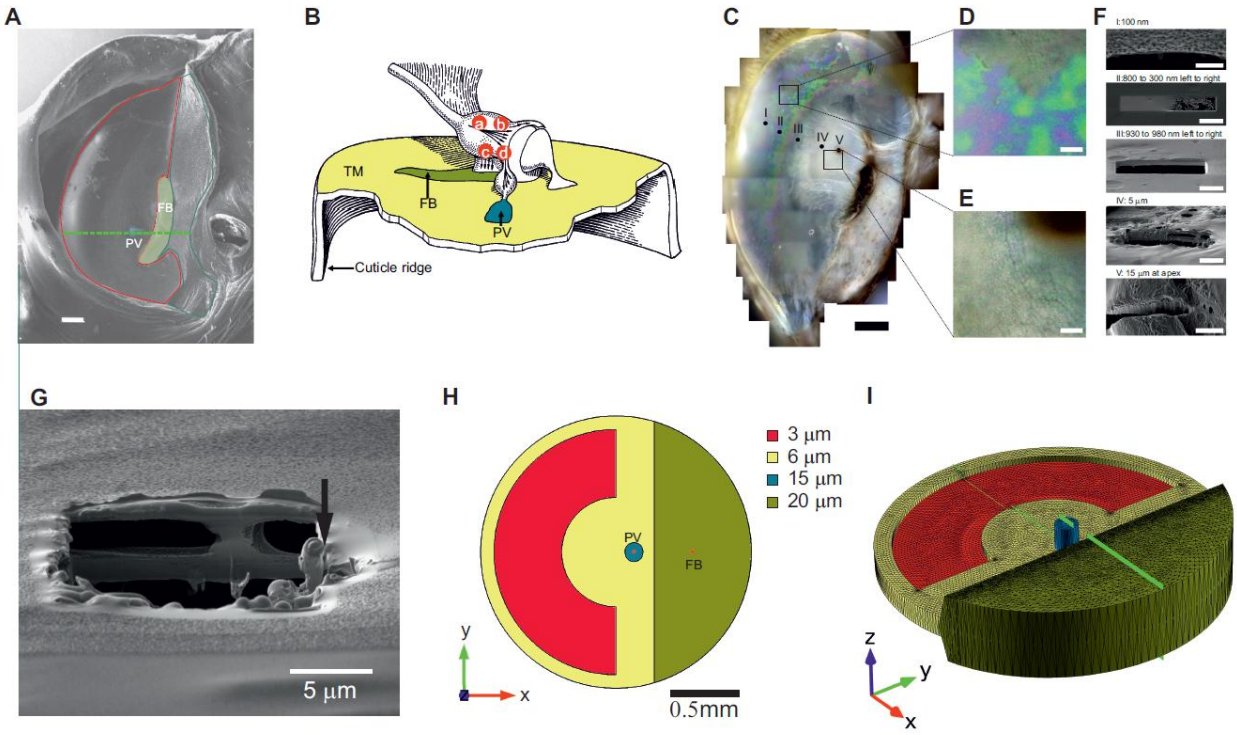

Figure 1C). These images also informed the selection of regions to investigate with the FIB milling.

3.3 Focused ion beam milling

Accelerated gallium ions were used to etch the TM with high precision at 5 selected locations. Freshly excised TMs were mounted, gold coated by plasma deposition and placed under vacuum (<2.5 µbar). A FIB milling station (FEI FIB201, Oregon, USA) was used to mill small trenches from which TM thickness could be measured.

3.4 Membrane response to acoustic stimulus

Real time velocity measurements of the vibrating TM were performed using time resolved laser Doppler vibrometry. No beads or reflective coating was necessary to obtain adequate laser reflection. The surface velocity was measured at many (minimum of ≈400 points) scan points across the tympanum in a radial arrangement about the PV. Previous studies showed that travelling flexural waves above 12 kHz had shorter wavelengths about the PV (5,9). Average velocity was calculated from 100 measurements made at each scan point. The ear was stimulated by sound at a single frequency for 4 cycles (5, 10, 15, 20, 25 kHz at 80 dB SPL (200 mPa)). Acoustic signals were generated by a waveform generator (Agilent 33120A, California, USA) amplified (Sony TAFE570, Tokyo, Japan) and fed to a Mylar leaf high dynamic range loudspeaker (ESS AMT-1, California, USA) positioned 30 cm from the ear. The SPL was measured using a calibrated 1/8th inch precision pressure microphone (Bruel & Kjaer 4138, Nærum, Denmark) and preamplifier (Bruel & Kjaer 2633). This reference microphone was positioned at ~10 mm from the tympanum. High coherence between microphone signal and mechanical response was achieved across the tympanum (>0.85) (shown in Supplementary Fig. 1). The transverse membrane velocity was measured optically using a microscanning LDV (Polytec PSV-300-F, Waldbronn, Germany) with an OFV-056

scanning head with close-up attachment. The laser spot of diameter ≈5 μm can be positioned with an accuracy of ≈1 μm. Laser vibrometry experiments were carried out on a vibration isolation table (TMC 784-443-12R, Massachusetts, USA) inside an acoustic isolation booth (IAC 1204A, New York, USA) at room temperature 24–26°C and relative humidity of 40–62%.

Polytec Software (Version 8.5, Waldbronn, Germany) was used to create out-of-plane spatial plots of velocity. Contour polar plots of kinetic energy density were created using POLAR3D program in Matlab 7.5 (The MathWorks Inc, Massachusetts, USA). Kinetic energy density, β, was calculated for each scan point using equation 3,

$$\beta = \tfrac{1}{2} h \mu V^2 \qquad (3)$$

where, V is the out-of-plane velocity and μ the density with a literature value of 1,300kg/m³ (14). The thickness, h, was estimated using a published thickness map which is more conservative than our measurements (15). To accurately measure the velocity of the travelling flexural waves across the membrane, the transverse velocity was recorded with high spatial resolution along a straight line through the FB and PV. These velocity data were integrated with respect to time to calculate displacement profiles along the scan line, using a custom made program written in Lab VIEW 8.0 (National Instruments, Texas, USA). An automated Gaussian curve-fitting program was written in Matlab 7.5 to track the position of the positive displacement peak of the travelling flexural wave at each time sample. The velocity of the travelling flexural wave along the scan line was then calculated by differentiating the peak position with respect to time.

3.5 Finite Element Analysis

A time dependent model of the TM was developed using COMSOL (COMSOL 4.3, Stockholm, Sweden). Our approach to creating the TM geometry was to use sectioning derived thickness measurements from literature (15) as well as FIB thickness measurements to create a simplified 3D geometry

(

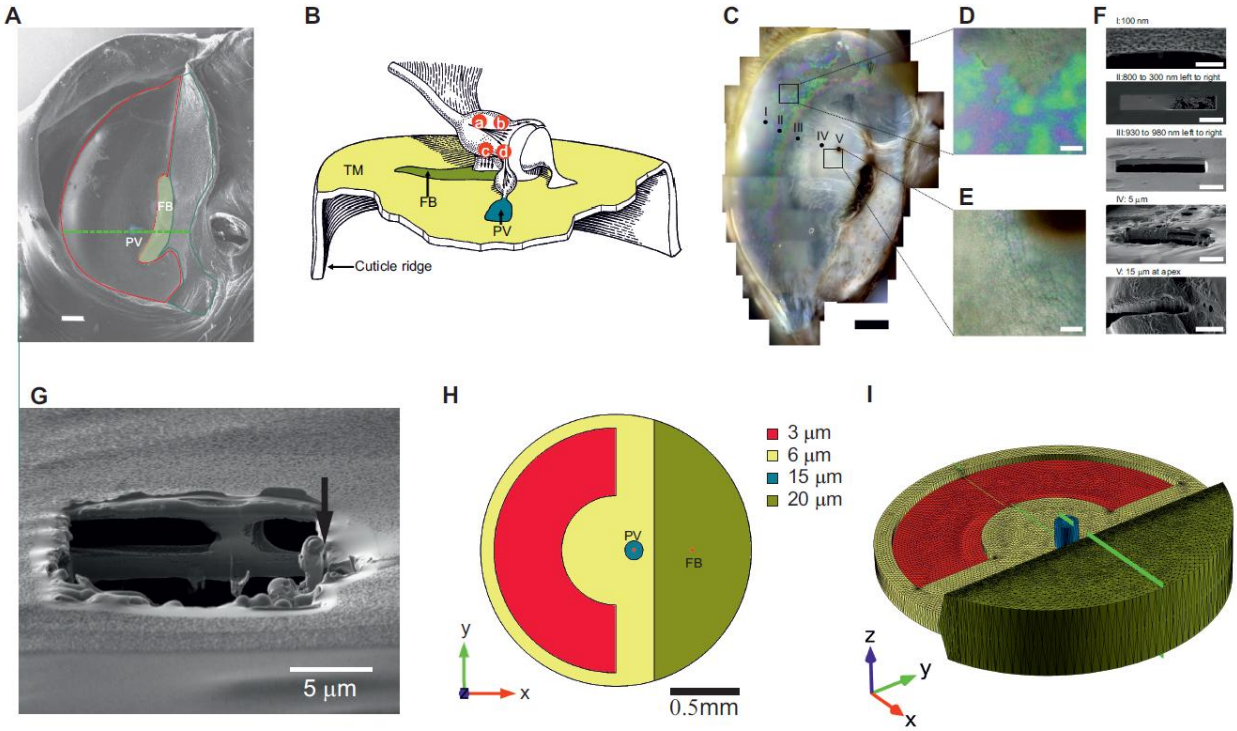

Figure 1I). The periphery of the TM was fully constrained as this was considered to be a suitable simulation of the sclerotised cuticle ridge. In effect, velocity measurements on the ridge are negligible. To ensure that the geometry was discretise with sufficient fidelity a mesh sensitivity study was conducted and it was observed that 64k elements were sufficient to capture the response of the membrane. An increase in mesh element number to 100k & 200k resulted in deflection differences of less than 1%, thus indicating a stable solution independent of mesh density. Similarly a time stepping sensitivity study was carried out.

The pre-strain in the model was captured by initially applying an in-plane displacement. A sinusoidal load (4 cycles, as per experiment) was then applied to the model membrane surface to simulate the acoustic surface loading (at a pressure of 200 mPa, and at 5, 10, 15, 20 & 25 kHz).

Given the absence of published material data for insect tympana, for a first approximation, the membrane was modelled as an isotropic linear elastic solid requiring only the density, Poisson's ratio and Young's modulus as material parameters. A density of 1,300 kg/m^3 was taken from literature (14). The Poisson's ratio was found to have little effect for values between 0.1-0.4, but has been shown by *Aernouts et. al.* to have an effect on membrane mechanics for values >0.4 (16). The commonly used value of 0.3 was used for the Poisson's ratio. As discussed previously, the real TM is known to be under pre-strain that needs to be considered for representative modelling.

Two quantities which are difficult to measure, but are required for modelling; pre-strain and Young's modulus. In effect, these two quantities are somewhat intractable as membrane stiffness is directly proportional to the tensile force, an effect known as 'stress stiffening' (17,18). As a consequence, a membrane with low intrinsic stiffness and high pre-strain behaves similarly to a membrane of high intrinsic stiffness and low pre-strain. Therefore without knowing one parameter, the other is also unknown. And thus far the measurement of either has proven very challenging. Here, a Young's modulus of 20 MPa was chosen as it has been used in other tympanic models (19). The strain was then chosen such that the

membrane deflections matched experimental values, resulting in strain of 1%, a value known to be modest compared to other known biological tissues (20). Rayleigh damping was used for all the FEA models with damping parameter values of α and β taken from literature (19). For frequency-independent models α=260 s^{-1} and β= 37 μs. For frequency-dependant damping models, α=260 s^{-1} and β ranged linearly from 37 to 74 μs for 5 & 25 kHz respectively. TM damping was formulated such that damping forces were directly proportional to the frequency of the acoustic stimulus. This assumption is based upon the principle of frequency dependent damping at a liquid-solid interface (21,22).

4 Results

4.1 Membrane microstructure

A key mechanical property of microphone diaphragms and TMs alike is membrane thickness. Previous measurements using a microtome method found that membrane thickness within an individual TM varies considerably, ranging from 0.6 to 20 μm (15). We used two approaches to study its thickness distribution in more detail; colour Newton ring interferometry

(

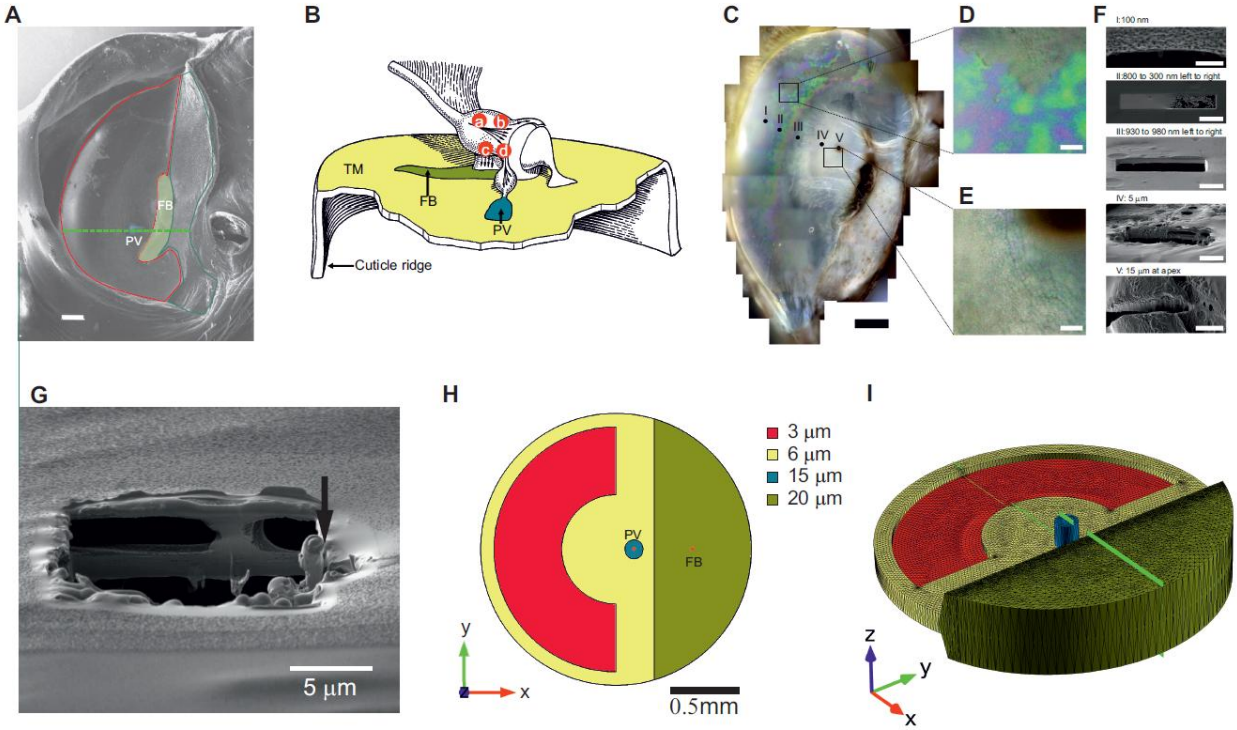

Figure 1C-E) and focused ion beam (FIB) milling

(

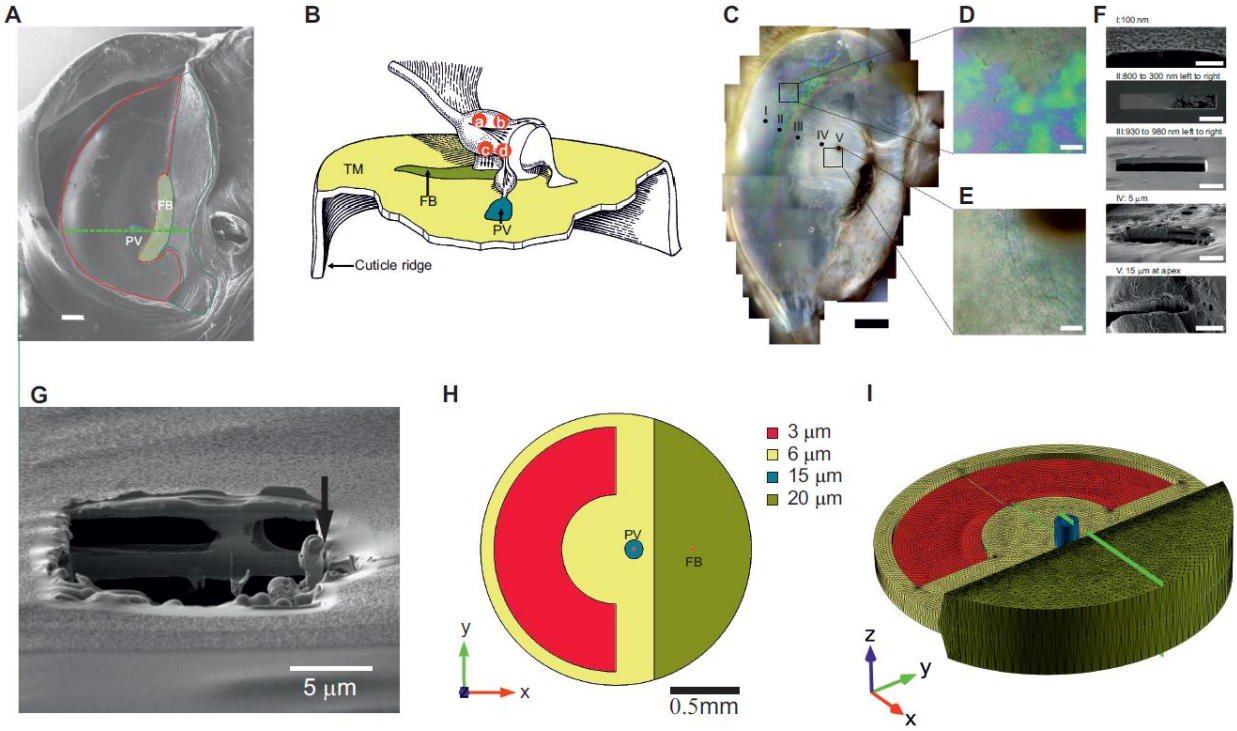

Figure 1F-G). The locust membrane presents a central thick region, containing neuronal attachment sites, and a surrounding roughly semicircular thin region

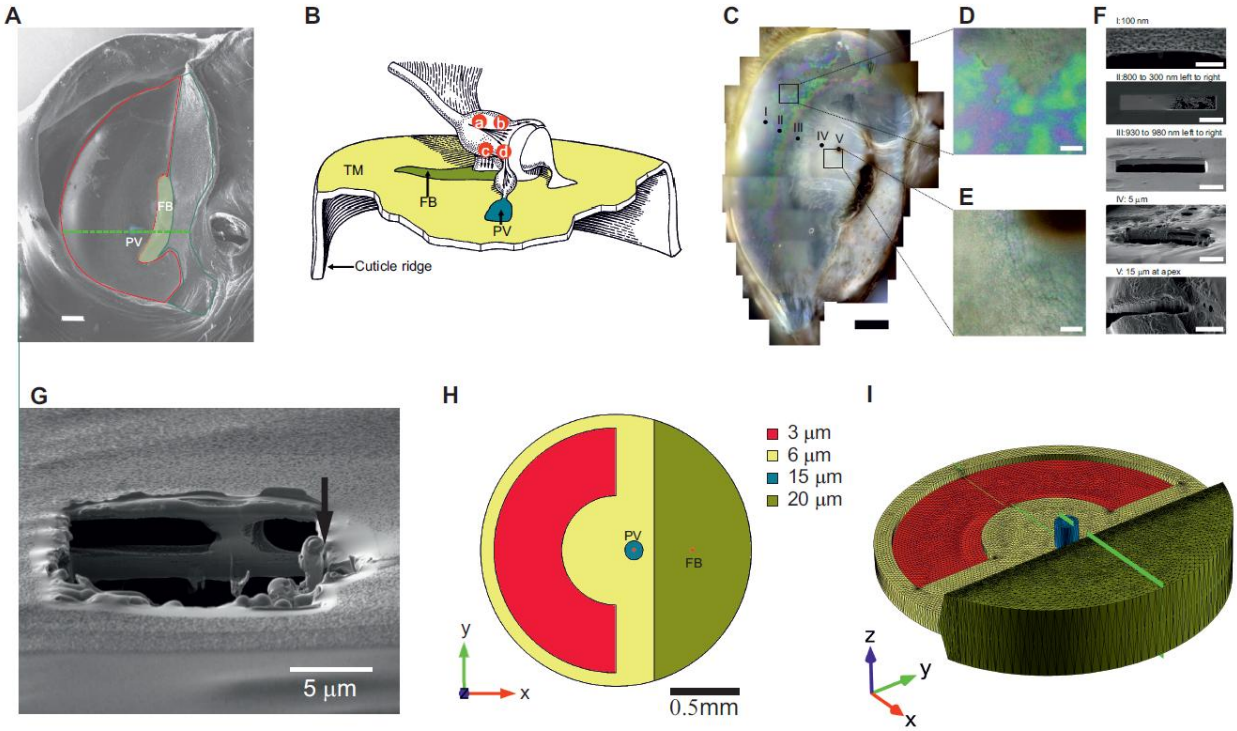

Figure 1. TM thickness ranges from approximately 100 nm in the thin region to 15 µm at the PV. At position IV, at the opaque region near the PV

(

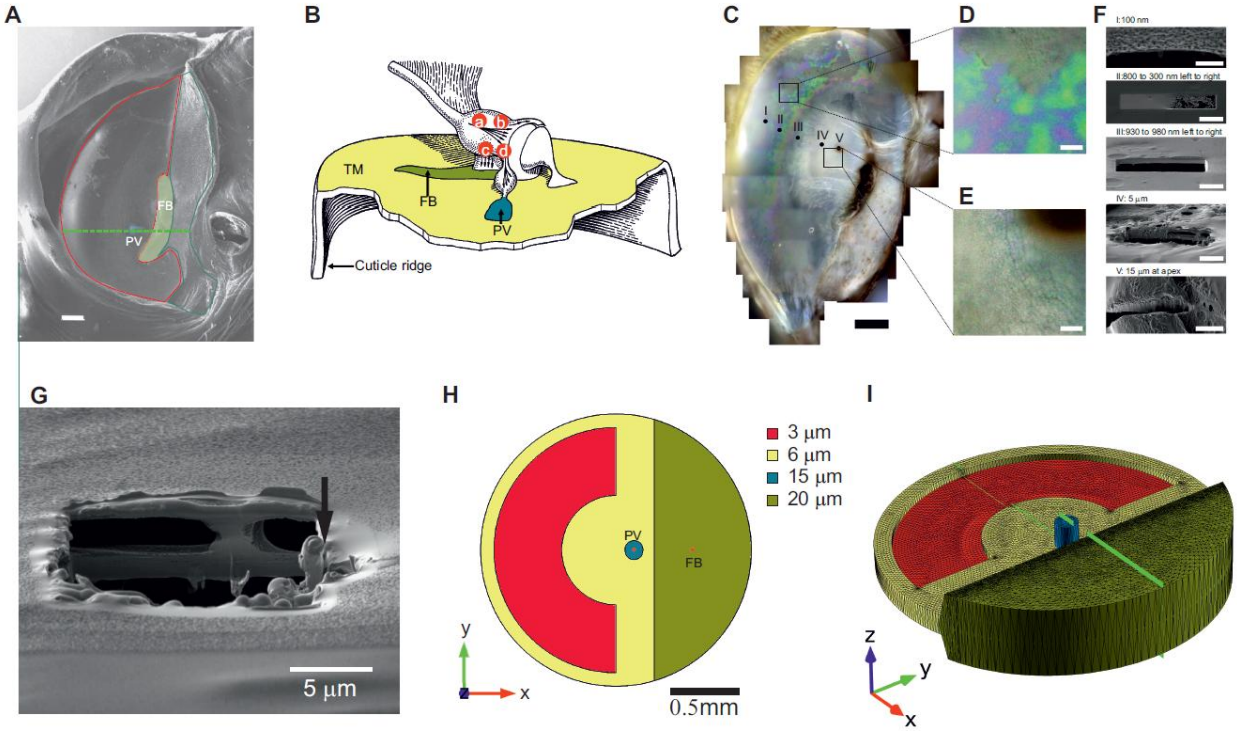

Figure 1C,E), the membrane is 5 µm thick, exhibiting internal cavities with bridging links between the internal and external surfaces

(

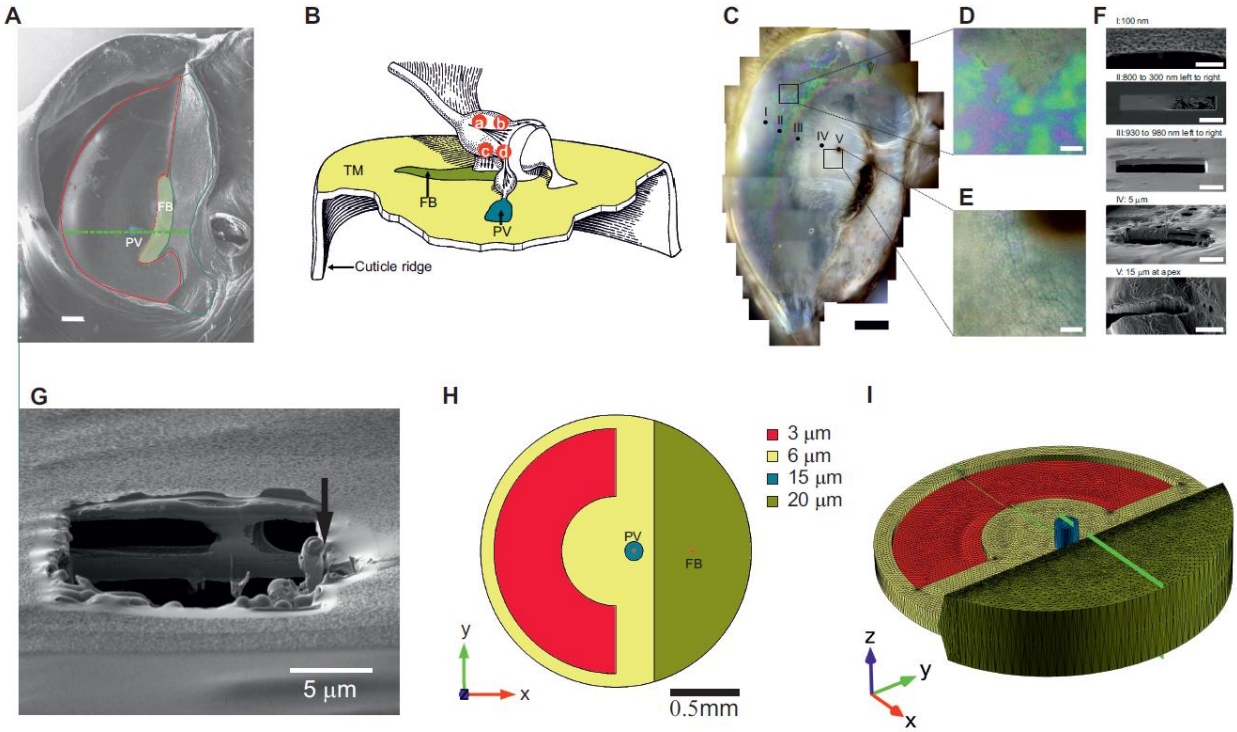

Figure 1G). Some local FIB redeposition artefacts are notable

(

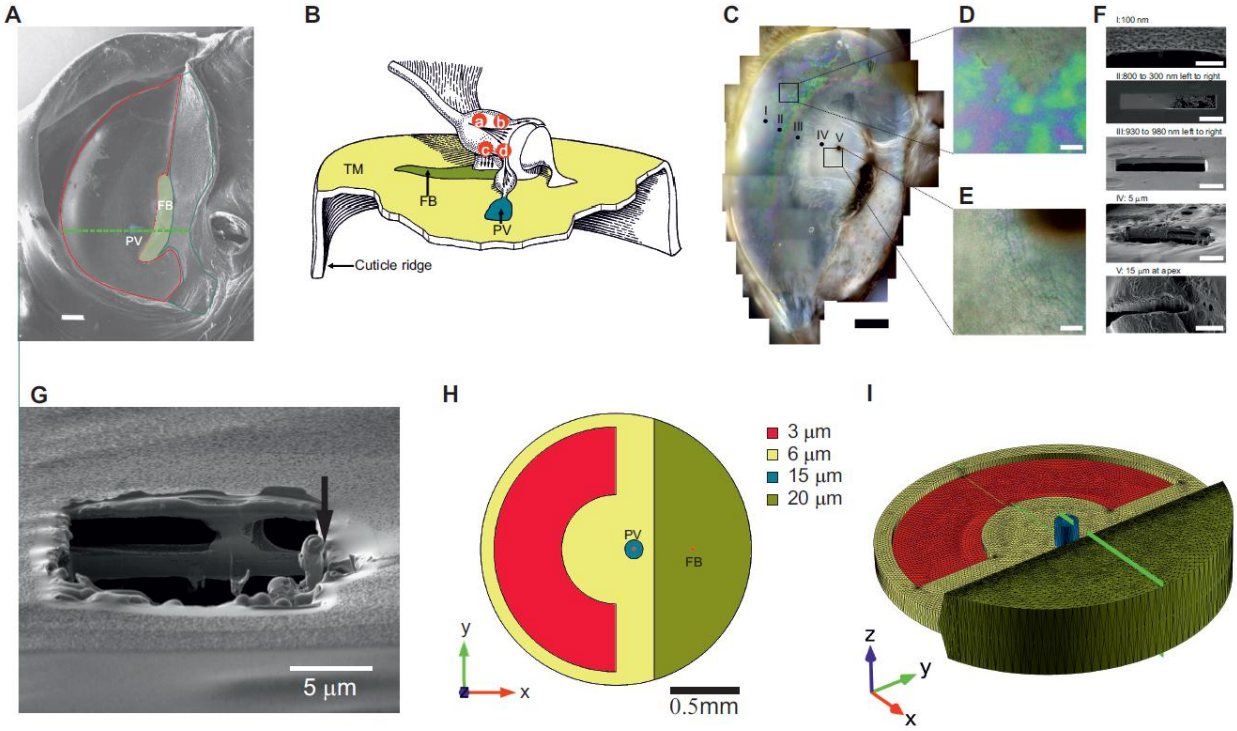

Figure 1G, Supplementary Fig. 2), likely resulting from liquids evaporating during cutting, suggesting that these cavities are fluid filled. Light microscopy imaging

(

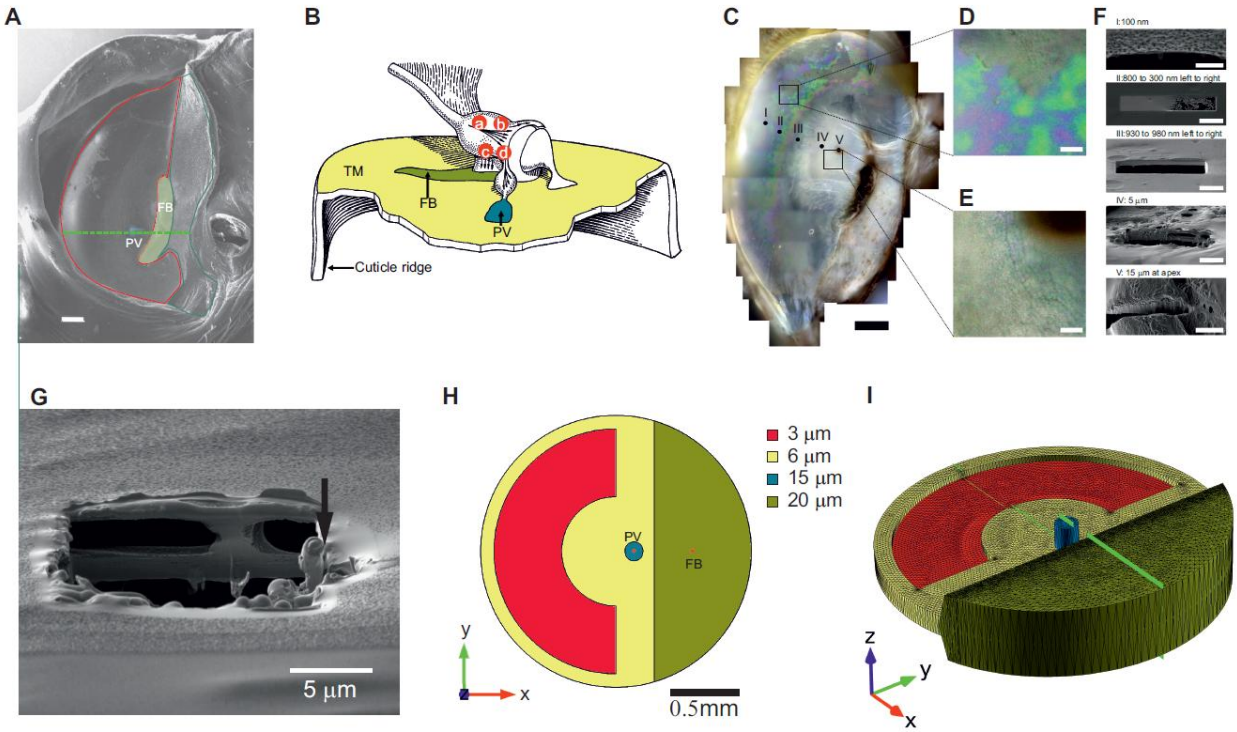

Figure 1D-E) also reveals that the white region (zone IV-V) has a compartmental structure

(

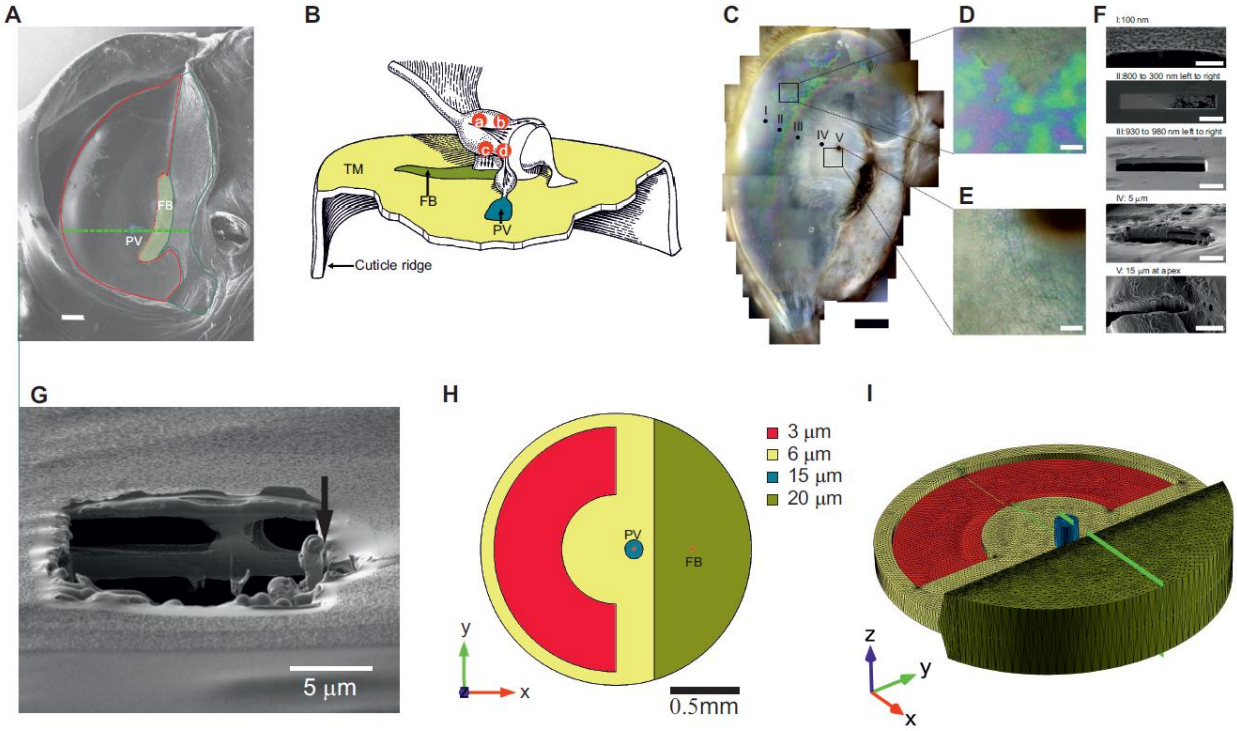

Figure 1E), supporting the presence of fluid filled chambers. The PV

(

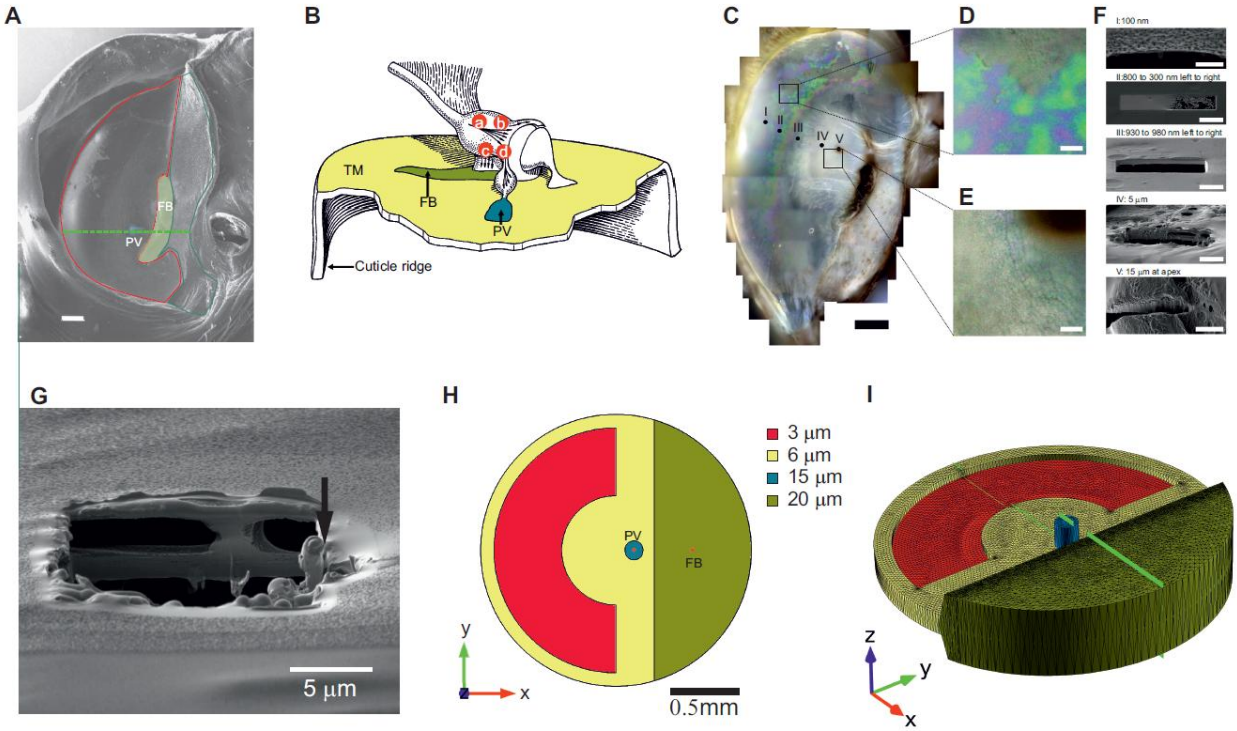

Figure 1C position V, E top right corner) is 15 µm thick at its apex; making it distinctly thicker than the surrounding membrane.

4.2 Tympanal response to acoustic stimuli and energy localisation

The TM's mechanical response was tested using tonal stimuli at different frequencies; 5, 10, 15, 10 & 25 kHz (example frequency response shown in Supplementary Fig. 3). For all frequencies, the initial TM displacement exhibits a semi-concentric travelling flexural wave developing in the thin region (Figure 2A, Movie 1). The travelling flexural wave subsequently converges on the PV and the thick region. The laser Doppler vibrometry measurements reveal that the travelling flexural wave slows down as it propagates towards the PV (Figure 3A), and its wavelength shortens, causing the deflection to increase in magnitude (Figure 3B,C). This is similar to wave shoaling, which occurs as sea waves approach shallower water at the shore (23).

To accurately quantify the velocity of the travelling flexural wave, we measured TM vibration displacement (normal to the surface) at high spatial resolution along a line in the established direction of wave propagation (Figure 3B). The peak of the travelling flexural wave was spatially tracked allowing the measurement of its propagation velocity. The velocity of the travelling flexural wave (Figure 3A) is relatively large in the thin region, where it first develops, and is notably frequency dependent. As the travelling flexural wave propagates towards the PV, propagation velocity decreases. This slowing behaviour is observed at all frequencies, except for 5-10 kHz, supporting the membrane hypothesis. For 15 kHz and above, wave velocity reduces to zero at the PV where propagation terminates. At 10 kHz, wave velocity slows down but is not zero. At 5kHz, however, the travelling wave traverses the PV without significant velocity reduction. This experimental analysis shows that in response to sound pressure, the TM's restorative force is principally due to membrane tension rather than stiffness. Altogether, this evidence indicates that tension is a key feature of tympanal function. It thus becomes apparent that real tympanal membranes most likely have a specific bending stiffness while also being under tension, as is the case for the FEA models that have both intrinsic stiffness and an applied tension.

An additional and important effect arising from the behaviour of TM travelling waves is the localisation of kinetic energy. In effect, the density of kinetic energy rises as the 15 kHz wave travels across the TM (Figure 2B). Quantitatively, kinetic energy (KE), rises from KE=2±0.5 at stimulus onset to 12±0.5 nJm^{-2} at the end of the stimulus. After one full oscillation period the KE is highly localised exactly at the PV. At 15 kHz, the shoaling-like behaviour results in the energy density at the PV to be two orders of magnitude higher than at any point on the thin membrane (Figure 4). A similar spatial pattern of energy localisation also takes place at frequencies above 15 kHz (Figure 4).

4.3 Finite Element Analysis

A simplified geometry based upon the real TM was derived, which captures the main TM structural characteristics: a thin semi-circular region, a surrounding area of average thickness, the PV and the thick FB region

(

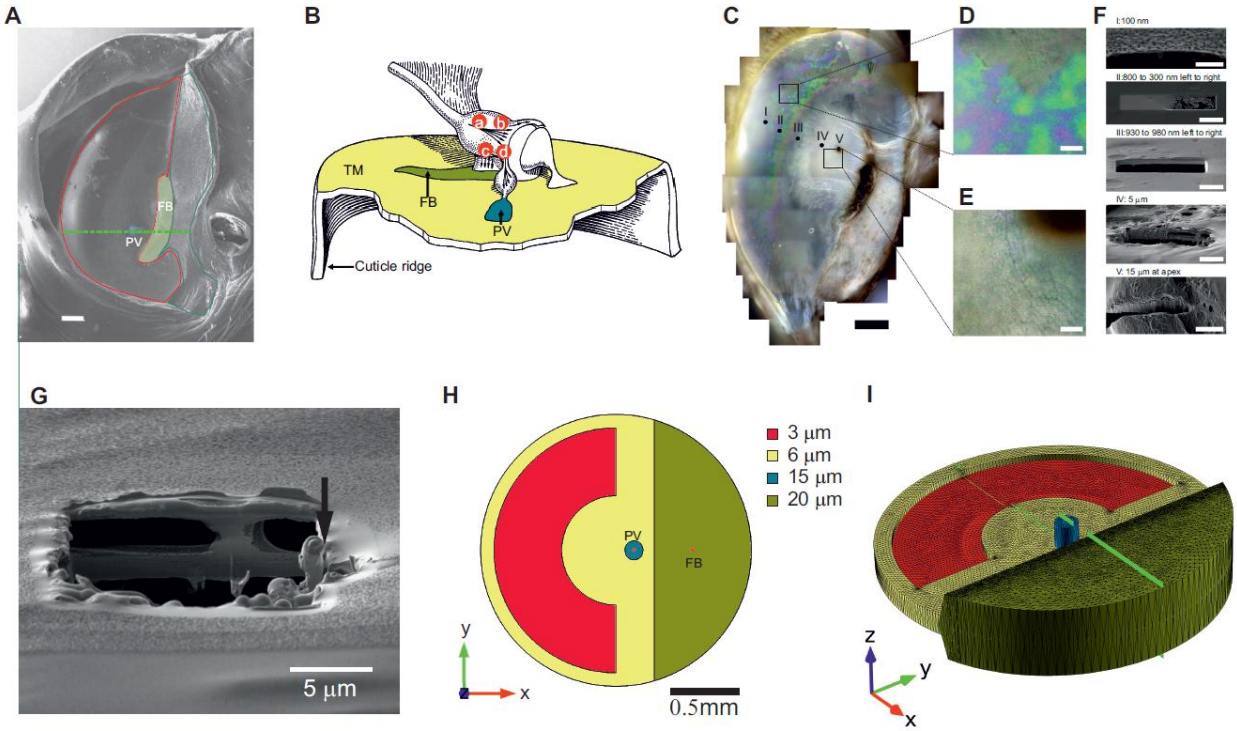

Figure 1H-I). Material properties were based on known tympana (see Methods). The FEA shows that a simple pre-tensioned, isotropic and linear elastic membrane is sufficient to capture all the main features of the real TM, namely; the generation of a travelling flexural wave, frequency decomposition and kinetic energy localisation.

As in the real TM, during the initial part of the sound stimulation (Figure 2C, φ <180°), a semi concentric wave is produced in the thinnest region of the FEA membrane, for all frequencies tested. The wave then travels across the membrane, and converges around the PV (Figure 2C, Movie 2). Flexural waves produced by lower frequencies (<10kHz) travel past the PV and reach the FB, similar in response to the real TM. When elicited by higher frequencies flexural waves are reduced in amplitude (Figure 3E). Thus, frequency decomposition is possible with this simulation and, as with the real locust tympanal membrane, the ratio of maximum PV to FB displacement increases for increasing frequency (Figure 5). The simulation is also able to capture the localisation of kinetic energy taking place at the PV, and with a topographical structure similar to the real TM (Figure 2D).

To the authors knowledge, pre-tension has as yet not been included in animal tympanum models (19,24–28) even though there is evidence of pre-tension existing in tympanic membranes (11,29,30). Recent research indicates that "prestrain plays a critical role in the mechanics of thin biological membranes" (31,32). In our computational models, the inclusion of membrane tension reveals that tension is a requirement for the presence of both flexural waves and kinetic energy localisation. Without the inclusion of membrane tension, the membrane behaves as a conventional vibrating plate without flexural wave propagation, frequency decomposition or kinetic energy localisation (Figure 5).

5 Discussion

The locust TM is structurally heterogeneous, a feature that distinguishes it from conventional microphone membranes. Collectively, data from spatially resolved Doppler vibrometry and FEA models suggest that variation in membrane thickness and tension produce two major effects. The gradient in compliance across the TM surface causes the thinner parts of the membrane to be more readily deflected by incoming sound energy. The semi-circular shape of this compliant part of the membrane causes the flexural wave to travel and converge towards its centre, causing an effective focusing of the acoustic energy captured by the membrane (Figure 2A-D). The increase in membrane thickness along the direction of travel of the flexural wave generates a second behaviour. Since in the locust TM the restoring force is dominated by tension, the flexural wave formed slows down as the membrane thickens, as shown in Equation 1. The reduction in this propagation velocity directly affects other wave parameters; the length of the flexural wave shortens and its amplitude increases. The consequence of the spatial convergence and shoaling of the flexural wave is a large deflection at the PV, which is located at the point of convergence (Figure 2A,C). The described mechanism is biologically relevant because it localises acoustic vibrational energy on to mechanoreceptors near the PV and therefore enhances the ear's sensitivity to sound. Two features define the locust TM; concentric shape of thickness gradient and tension dominated mechanics. These features, when combined, improve hearing sensitivity. Interestingly, a similar distribution of thickness has also been observed in mammalian tympana (33–35).

Location specific frequency decomposition is a purely mechanical effect of the wavelength of the travelling flexural wave interacting with the particular structure of the TM. At high frequencies, the wavelength of the travelling flexural wave is smaller than the dimensions of the TM, therefore flexural wave velocity will be dependent on the thickness at a smaller spatial scale, while wave speed and shape will be susceptible to local thickness gradients. In contrast, for long wavelengths, the effective thickness experienced by the flexural wave is the average thickness over that larger distance, thus making it impervious to local thickness gradients. We propose that the long wavelength of the travelling flexural wave at 5 kHz averages out local changes in membrane thickness and produces a nearly constant velocity. By a similar argument, the strong frequency dependence of travelling flexural wave velocity at the start of propagation could occur because higher frequencies have smaller wavelengths and hence are more sensitive to the local changes in membrane thickness.

The TM is structurally complicated; FEA enables the incorporation of structural complexity into functional models testing the conjecture that material properties, concentric thickness gradients and tension together produce the observed mechanical response.

However, in formulating the FEA model, certain simplifying assumptions are necessary, and here we unfold their implications. For instance, tympanal membranes are usually modelled in an isotropic linear-elastic regime (19,36–38) even though they are probably anisotropic and viscoelastic (39). Given the difficulty of dynamic material characterisation, using an isotropic linear elastic regime often proves to be an acceptable first approximation, as validated by the present locust TM model. Ignoring the contribution of tension (19,26), these models only indirectly account for the behaviour by way of the stress-stiffening effect (10). The evidence presented, using experimental, mathematical and FEA approaches, suggests tension is a crucial factor in the generation of the full range of mechanical behaviour.

Another assumption pertains to the damping behaviour of the liquid-filled chambers observed in some regions of the TM (

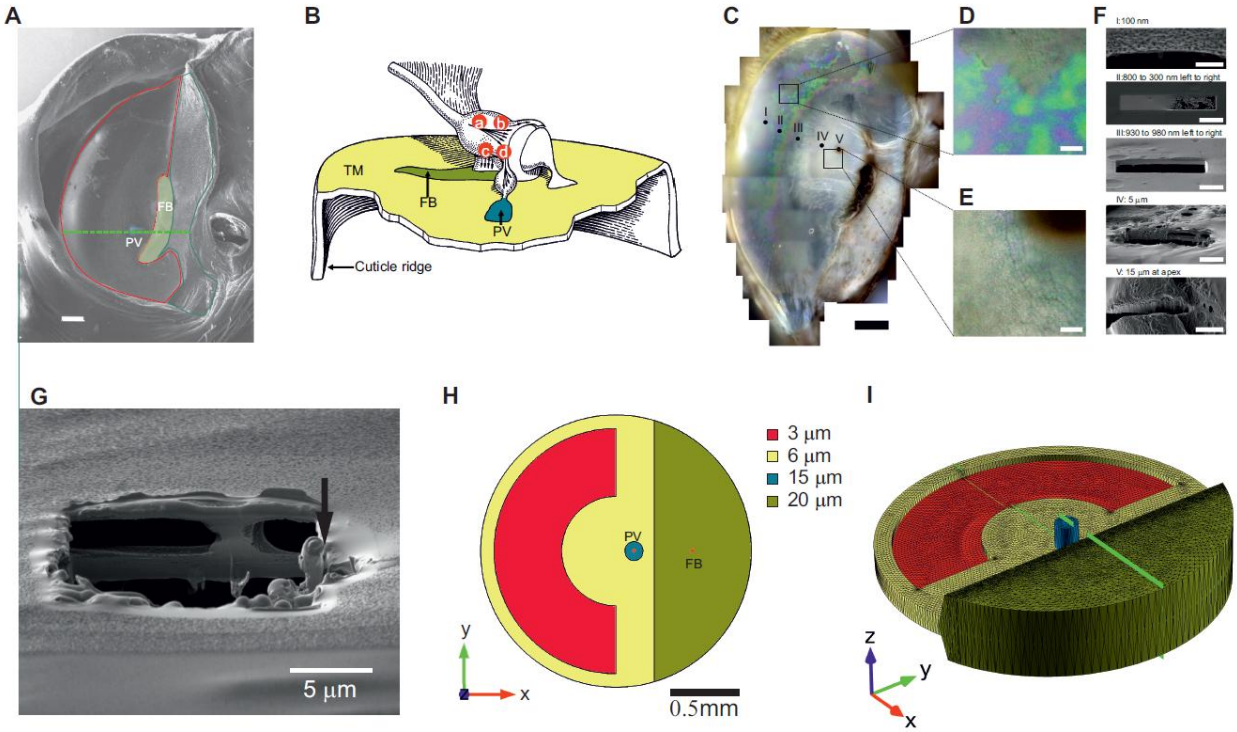

Figure 1G). Previous work has suggested that the damping experienced by flexural waves at a liquid-solid interface increases with frequency (21,22). Here, damping is found to enable the membrane to terminate flexural waves, and in a frequency-dependent manner. Yet, models where the damping forces are independent of frequency can still explain frequency dependent localisation (Figure 5). Such models can behave like the locust TM when the thickness of the thick region is scaled by a factor of three, or more. This adaptation is sufficient to produce frequency localisation even in the absence of frequency dependent damping (Figure 5). Notably such a three-fold change results an increase in membrane stiffness by a factor of 27, as flexural stiffness is proportional to the cube of thickness. Such stiffening would thus reduce the deflection magnitude of the membrane for a given pressure, likely reducing the mechanical sensitivity of the hearing organ.

The liquid-filled partitions surrounding the PV

(

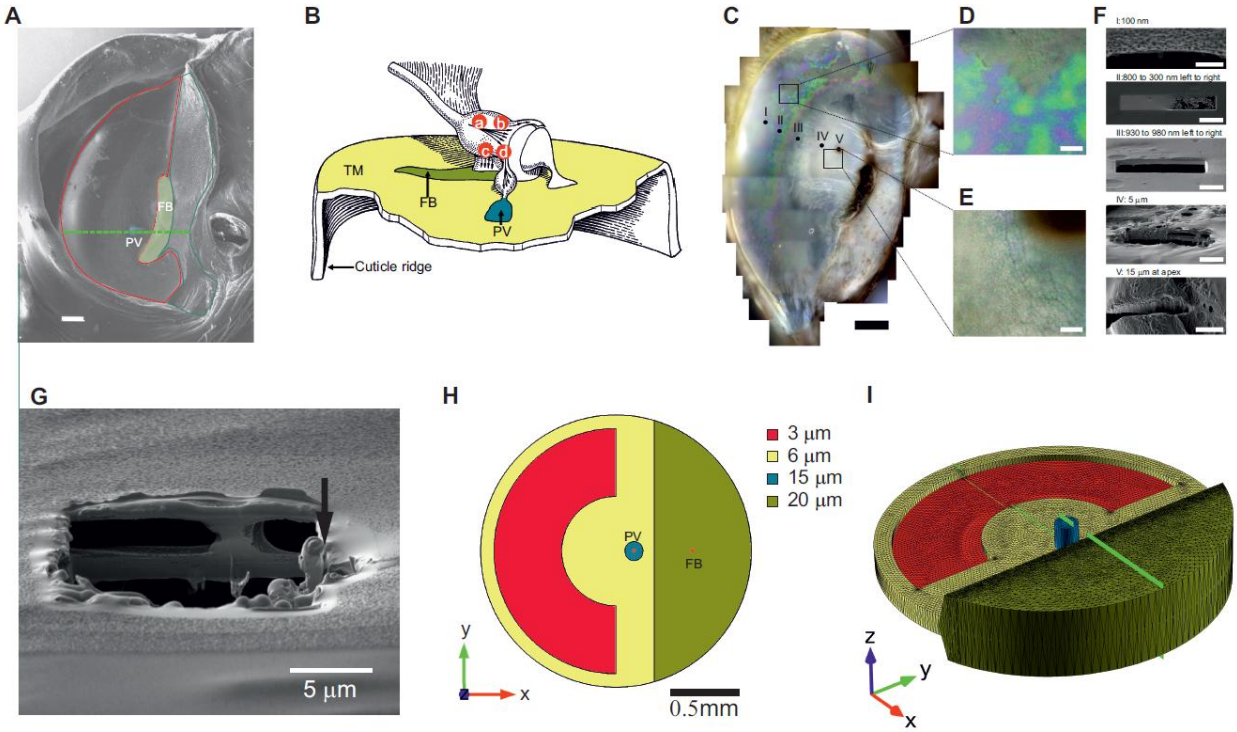

Figure 1G) seem to be implicated in the mechanism of frequency discrimination. This assertion is supported by experiments on excised membranes that do not show the frequency-dependent travelling waves observed in *in-situ* membranes (15). We conjecture that this change in mechanical response is caused by the collapse of the fluid-solid interface, generating substantial changes in TM damping properties (40–42). The FEA results show that the structural mechanism underlying this response is robust and can be readily generalised. There is therefore an opportunity for designing a new type of sound sensor based on the principles at work in the locust tympanal membrane.

Conventionally, microphones are designed to prevent the formation of travelling flexural waves across their diaphragm. Such mechanical response is deemed undesirable, as it alters the sought-after flat frequency response. The energy localisation observed in the locust, and the proposed mechanism, may be of interest to a different microphone design as it would allow transduction to take place at a location of maximum deflection. Further along, an array of such membranes can be imagined that would serve as a sensitive mechanical frequency analyser, powered by sound energy only. Such solution to acoustic frequency analysis constitutes an alternative to conventional digital signal processing, and to the mechanisms found in the mammalian cochlea.

6 References

1. Kurokawa H, Goode RL. Sound pressure gain produced by the human middle ear. Otolaryngology--head and neck surgery : official journal of American Academy of Otolaryngology-Head and Neck Surgery. 1995 Oct;113(4):349–55.

2. Yack JE. The structure and function of auditory chordotonal organs in insects. Microscopy research and technique. 2004 Apr 15;63(6):315–37.

3. Montealegre-Z F, Jonsson T, Robson-Brown KA, Postles M, Robert D. Convergent evolution between insect and mammalian audition. Science (New York, N.Y.). 2012 Nov 16;338(6109):968–71.

4. Hoy RR, Robert D. Tympanal hearing in insects. Annual review of entomology. 1996 Jan;41:433–50.

5. Windmill JFC, Bockenhauer S, Robert D. Time-resolved tympanal mechanics of the locust. Journal of the Royal Society, Interface / the Royal Society. 2008 Dec 6;5(29):1435–43.

6. Gray EG. The Fine Structure of the Insect Ear. Philosophical Transactions of the Royal Society of London B- Biological Sciences. 1960;243(700):10–94.

7. Jacobs K, Otte B, Lakes-Harlan R. Tympanal receptor cells of Schistocerca gregaria: Correlation of soma positions and dendrite attachment sites, central projections and physiologies. Journal of Experimental Zoology. 1999 Feb 15;283(3):270–85.

8. Römer H. Processing of information by tympanal receptors of Locusta migratoria (Acrididae, Orthoptera). Journal of comparative physiology. 1976;109(1):101–22.

9. Windmill JFC, Göpfert MC, Robert D. Tympanal travelling waves in migratory locusts. The Journal of experimental biology. 2005 Jan;208(Pt 1):157–68.

10. Voorthuyzen JA, Bergveld P. The influence of tensile forces on the deflection of circular diaphragms in pressure sensors. Sensors and Actuators. 1984 Nov;6(3):201–13.

11. Michelsen A. The physiology of the locust ear. Journal of Comparative Physiology A. 1971 Mar;71(1):102–28.

12. Meyer J, Hedwig B. The influence of tracheal pressure changes on the responses of the tympanal membrane and auditory receptors in the locust Locusta migratoria. Journal of Experimental Biology. 1995;198(6):1327–39.

13. Brekhovskikh L, Goncharov V. Mechanics of continua and wave dynamics. Berlin and New York: Springer-Verlag; 1985.

14. Wainwright SA, Biggs WD, Currey JD, Gosline JM. Mechanical Design in Organisms. London: Princeton Univeristy Press; 1982. p. 423.

15. Stephen RO, Bennet-Clark HC. The anatomical and mechanical basis of stimulation and frequency analysis in the locust ear. Journal of Experimental Biology. 1982;99(8):279–317.

16. Aernouts J, Soons JAM, Dirckx JJJ. Quantification of tympanic membrane elasticity parameters from in situ point indentation measurements: validation and preliminary study. Hearing research. 2010 May;263(1-2):177–82.

17. Thorin A, Azoug A, Constantinescu A. Influence of prestrain on mechanical properties of highly-filled elastomers: Measurements and modeling. Polymer Testing. 2012 Dec;31(8):978–86.

18. Bonet J, Wood RD. Nonlinear continuum mechanics for finite element analysis. 2nd ed. Cambridge, England: Cambridge Univeristy Press; 2008.

19. Volandri G, Di Puccio F, Forte P, Carmignani C. Biomechanics of the tympanic membrane. Journal of biomechanics. 2011 Apr 29;44(7):1219–36.

20. Meyers MA, Chen PY, Lin AYM, Seki Y. Biological materials: Structure and mechanical properties. Progress in Materials Science. 2008;53:1–206.

21. Weinberg MS, Dube CE, Petrovich A, Zapata AM. Fluid damping in resonant flexural plate wave device. Journal of Microelectromechanical Systems. 2003 Oct;12(5):567–76.

22. Gubaidullin AA, Kuchugurina OY, Smeulders DMJ, Wisse CJ. Frequency-dependent acoustic properties of a fluid/porous solid interface. The Journal of the Acoustical Society of America. 2004;116(3):1474.

23. Longuet-Higgins MS, Stewart RW. Radiation stress in water waves, a physical discussion with applications. Deep Sea Research. 1964;11:529–62.

24. Aernouts J, Dirckx JJJ. Static versus dynamic gerbil tympanic membrane elasticity: derivation of the complex modulus. Biomechanics and modeling in mechanobiology. 2012 Jul;11(6):829–40.

25. Aernouts J, Aerts JRM, Dirckx JJJ. Mechanical properties of human tympanic membrane in the quasi-static regime from in situ point indentation measurements. Hearing research. 2012 Aug;290(1-2):45–54.

26. Elkhouri N, Liu H, Funnell WRJ. Low-frequency finite-element modeling of the gerbil middle ear. Journal of the Association for Research in Otolaryngology : JARO. 2006 Dec;7(4):399–411.

27. Zhao F, Koike T, Wang J, Sienz H, Meredith R. Finite element analysis of the middle ear transfer functions and related pathologies. Medical engineering & physics. 2009 Oct;31(8):907–16.

28. Salamati E, Agrawal S, Samani A, Ladak H. Estimation of the Orthotropic Elastic Properties of the Rat Eardrum. Journal of Medical and Biological Engineering. 2012;32(4):225–34.

29. Ichiro K. The structure and function of the middle ear. Tokyo: Univeristy of Tokyo Press; 1960.

30. Békésy G. Experiments in Hearing. 1st ed. Toronto: McGraw-Hill; 1960.

31. Rausch MK, Kuhl E. On the effect of prestrain and residual stress in thin biological membranes. Journal of the Mechanics and Physics of Solids. 2013 May;In press.

32. Rausch MK, Famaey N, Shultz TO, Bothe W, Miller DC, Kuhl E. Mechanics of the mitral valve : A critical review, an in vivo parameter identification, and the effect of prestrain. Biomechanics and modeling in mechanobiology. 2012 Dec 21;

33. Kuypers LC, Dirckx JJJ, Decraemer WF, Timmermans J-P. Thickness of the gerbil tympanic membrane measured with confocal microscopy. Hearing research. 2005 Nov;209(1-2):42–52.

34. Kuypers LC, Decraemer WF, Dirckx JJJ. Thickness distribution of fresh and preserved human eardrums measured with confocal microscopy. Otology & neurotology : official publication of the

American Otological Society, American Neurotology Society [and] European Academy of Otology and Neurotology. 2006 Feb;27(2):256–64.

35. Kuypers LC, Decraemer WF, Dirckx JJJ, Timmermans J-P. Thickness distribution of fresh eardrums of cat obtained with confocal microscopy. Journal of the Association for Research in Otolaryngology : JARO. 2005 Sep;6(3):223–33.

36. Liu Y, Li S, Sun X. Numerical analysis of ossicular chain lesion of human ear. Acta Mechanica Sinica. 2008 Nov 11;25(2):241–7.

37. Le CD, Huynh QL. Mathematical models of human middle ear in chronic otitis media. 2008 International Conference on Technology and Applications in Biomedicine. IEEE; 2008. p. 426–9.

38. Ladak HM, Funnell WRJ, Decraemer WF, Dirckx JJJ. A geometrically nonlinear finite-element model of the cat eardrum. The Journal of the Acoustical Society of America. 2006;119(5):2859.

39. Fung YC. Biomechanics: Mechanical Properties of Living Tissues. 2nd ed. New York: Springer; 1993.

40. Vincent JF V. Deconstructing the design of a biological material. Journal of theoretical biology. 2005 Sep;236(1):73–8.

41. Barthelat F, Tang H, Zavattieri P, Li C, Espinosa H. On the mechanics of mother-of-pearl: A key feature in the material hierarchical structure. Journal of the Mechanics and Physics of Solids. 2007 Feb;55(2):306–37.

42. Klocke D, Schmitz H. Water as a major modulator of the mechanical properties of insect cuticle. Acta biomaterialia. 2011 Jul;7(7):2935–42.

Acknowledgments

NM is supported by a Marie Curie fellowship. DR is supported by the Royal Society of London and the Wolfson Foundation. The project was funded by a grant from the Biotechnology and Biological Sciences Research Council UK.

Author contribution

RM, TRM, NM & DR wrote the paper. TRM conducted thin film interferometry, vibrometry and analysis of results, and formulated mathematical models. NM conducted FIB milling and analysis & analysed vibrometry data. TSS conducted FIB milling and analysis. RM conducted FEA modelling and analysis. DR oversaw research.

Figures

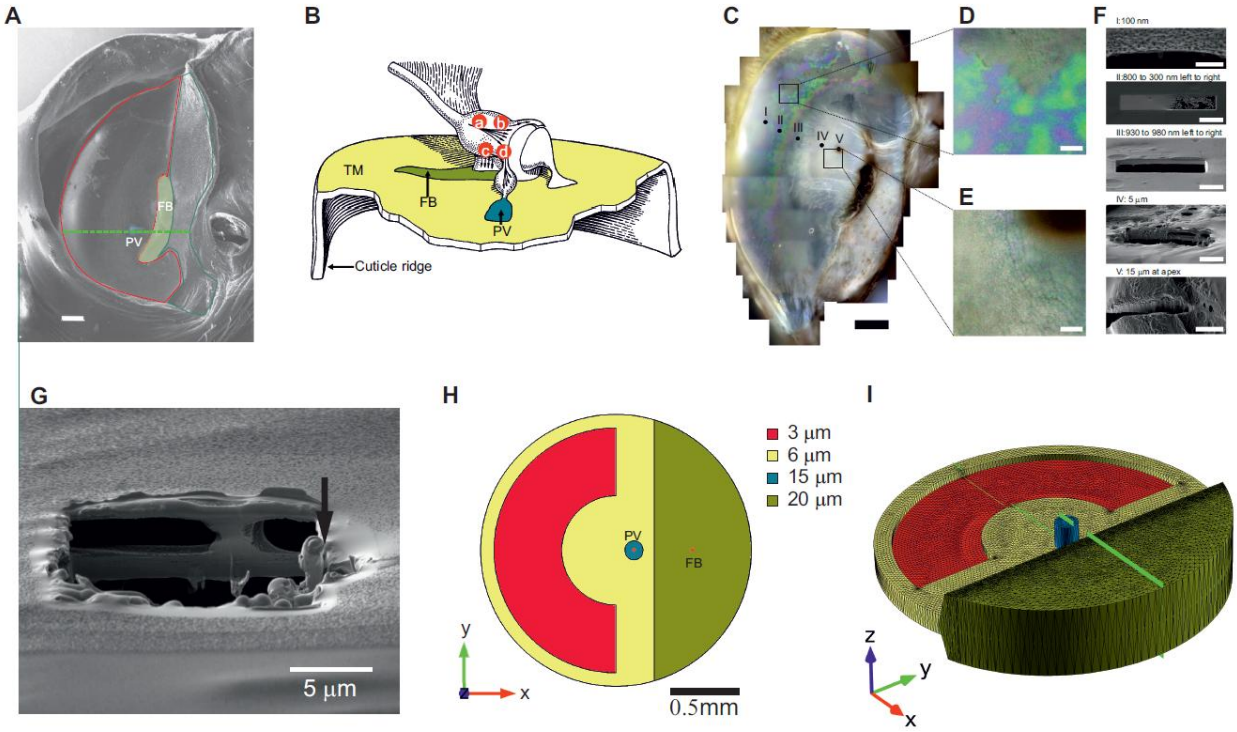

Figure 1 - Locust membrane, FIB milling of internal structure and FEA geometry. (A)SEM of external ear surface, thin region outlined in red, thick region in green, folded body (FB) in solid green, pyriform vesicle (PV) in solid blue and dashed green line showing transect. (B) Inner surface of the locust ear showing receptor cell groups (a,b,c for low frequency and d for high frequency) in Müller's organ attached to the TM and cuticle ridge, adapted from (6)**. (C) Newton ring interferometry of membrane. (D) Thin region. (E) PV. (F) FIB millings at locations shown in (C). (G) Enclosed fluid filled chambers (the arrow indicates an artefact formed by the redeposition of liquid during FIB milling. Another section is shown in detail in Supplementary Fig 2.). (H) Geometry and thickness of FEA membrane model. (I) Scaled geometry of FEA model showing green transect line. [Scale bars: (A)(C) 200 µm, (D)(E) 20 µm, (F-I) 2 µm, (F-II,III,IV,V) 20 µm.]**

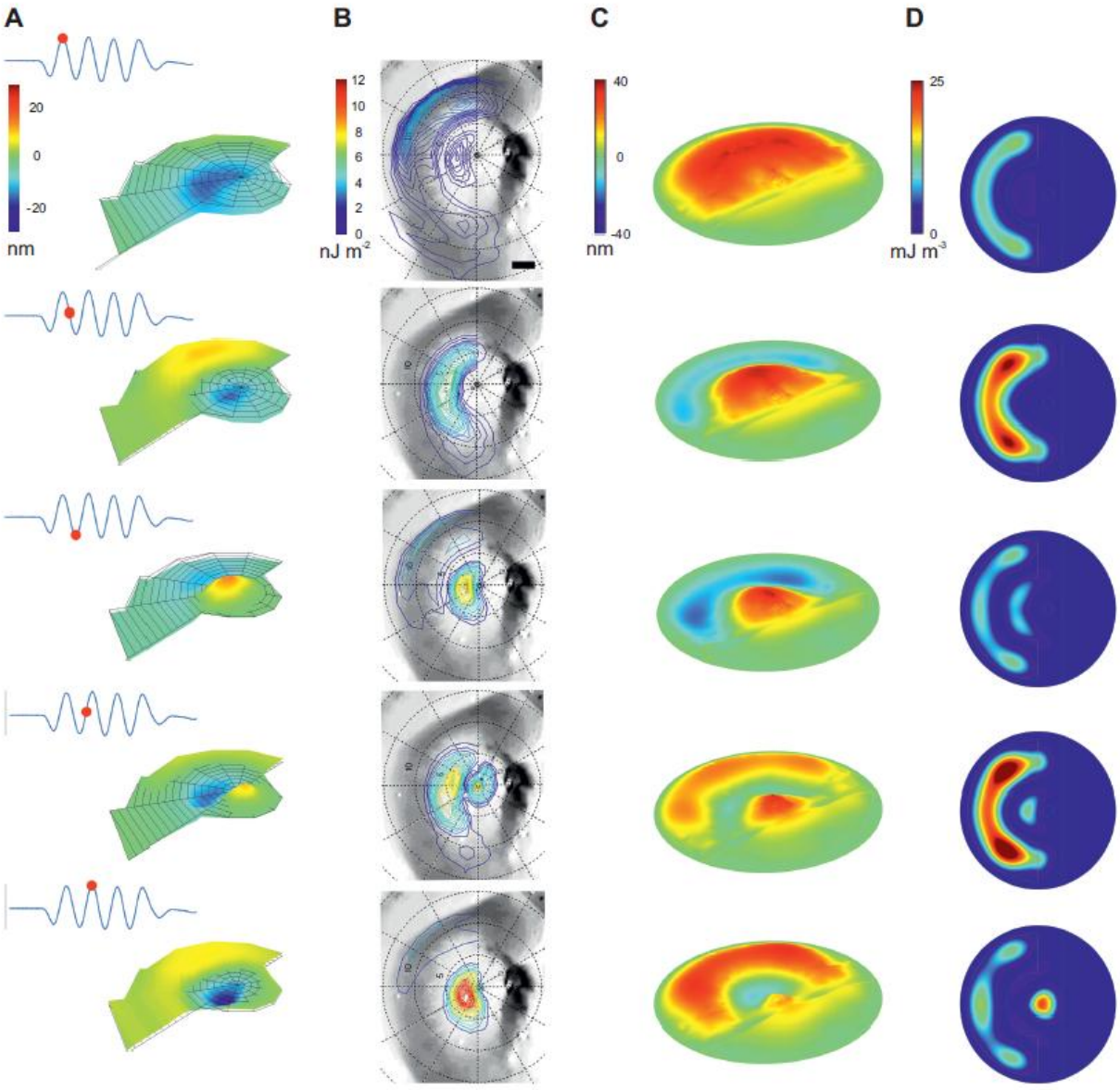

Figure 2 - Deflection shapes and energy density plots at equal time points for real and FEA membranes: (A) Scaled deflection plots of membrane at phase intervals of 90° with respect to first positive pressure peak of a 15 kHz sinusoidal pulse train. (B) Corresponding kinetic energy density. (C) Scaled FEA membrane deflection shapes. (D) Kinetic energy density plots of FEA model. Scale bars (B)(D): 500 µm. Real membrane 2.5 x 1.5mm, FEA membrane 2 x 2mm.

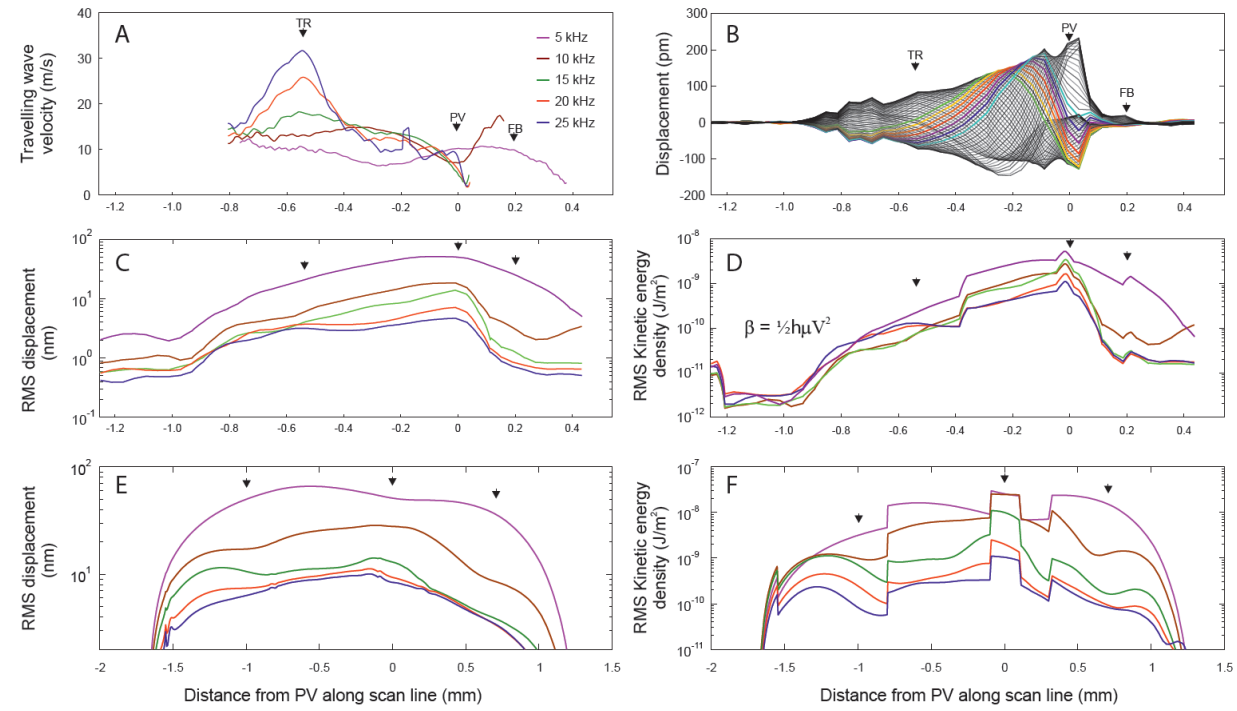

Figure 3 - Membrane response along transect lines. Real membrane (A)-(D), FEA membrane (E)-(F). (A) Flexural wave velocity. (B) Membrane deflection at 15 kHz at a selection of time intervals. Coloured deflection curves show increasing deflection magnitude with time. (C)+(E) RMS displacements. (D)+(F) RMS kinetic energy. The arrows mark the positions of the TR: Thin region, PV: pyriform vesicle, FB: folded body in the plots.

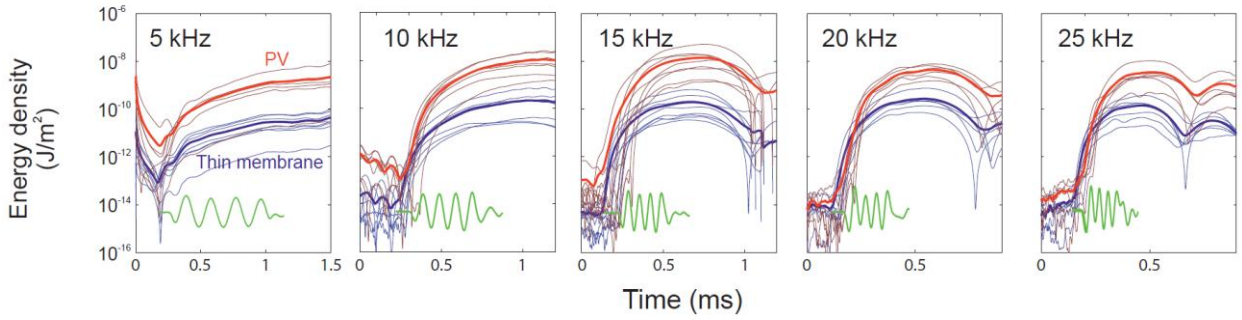

Figure 4 - Kinetic energy density along transect as a function of time. Insert: Corresponding time evolution of stimulation impulse train.

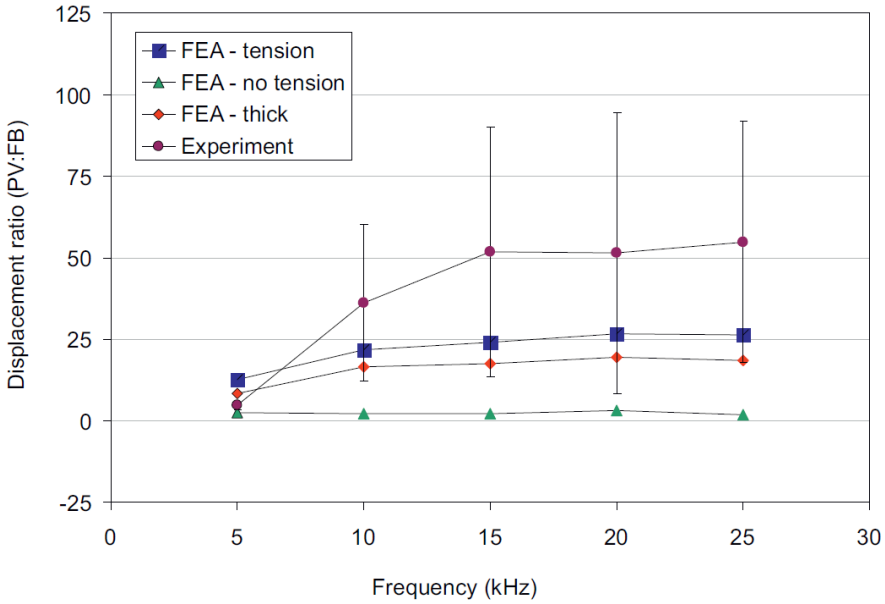

Figure 5 - Frequency discrimination as defined as a ratio of peak membrane deflection at the PV and FB. FEA models show vital role of membrane tension in frequency decomposition. FEA model without frequency dependent damping (FEA - thick) shows frequency discrimination can be achieved by increasing thickness of thick portion of the membrane. Real membranes show significant variance in response.

Movie 1 – Animation of real membrane deflection shape captured using time resolved vibrometry. The deflection has been scaled significantly to show flexural wave evolution. Excitation at 15 kHz.

Movie 2 – Animation of membrane deflection of FEA model. As with Movie 1 the out of plane deflection has been scaled significantly. Excitation at 15 kHz.